Chemistry–A European Journal
Research Article
doi.org/10.1002/chem.202301958
Chemistry Europe
European Chemical Societies Publishing
www.chemeurj.org

Hot Paper

Special Collection

Diverse Reactions of Formazanate/Formazan with Tetrylenes: Reduction, C–H Bond Activation, Substitution and Addition

Da Jin,[a] Xiaofei Sun,[a] Vanitha R. Naina,[a] and Peter W. Roesky*[a]

Dedicated to Professor Hansjörg Grützmacher, Professor Evamarie Hey-Hawkins, Professor Manfred Scheer, and Professor Werner Uhl.

The reactivity of the formazanate potassium salt [L^{tBu}K(thf)] (L^{tBu}=PhNNC(4-^{t}BuPh)NNPh) with the group 14 chlorotetrylenes [{PhC(^{t}BuN)$_2$}ECl] (E=Si, Ge, Sn) was investigated. Three corresponding compounds with unique configurations were formed, demonstrating the diverse reactivity of the system. In addition to the anticipated salt metathesis reactions of the potassium salt with the chlorine function of tetrylenes, unexpected reduction/insertion steps into the N=N bond of the formazanate (Si, Ge) and subsequent C–H activation (Ge) were also observed. Furthermore, when the neutral formazan ligand [L^{tBu}H] was exposed to silylenes [{PhC(^{t}BuN)$_2$}SiCl] and [L^{Ph}SiNMePy], substitution and addition reactions occurred. These discoveries significantly enrich the diversity of formazanate/formazan redox chemistry, opening up new avenues for exploration in this field.

Introduction

Formazans, a class of nitrogen-rich compounds featuring a –NH–N=C–N=N– backbone,[1] have gained significant attention for their applications in textile dyes[2–4] and chemical biology.[5–7] Furthermore, formazanates, derived from the deprotonation of formazans, exhibit distinctive characteristics as monoanionic chelating ligands. While formazanates are often compared to β-diketiminate ligands, they possess unique electronic properties.[8] The presence of four nitrogen atoms in the backbone grants formazanates a low-energy LUMO, enabling ligand-based reductive activations of coordinated compounds under mild conditions.[9–11] Extensive research has focused on the redox-active nature of formazanates, including the reduction of corresponding metal complexes using $CoCp_2$ (Cp = cyclopentadienide) or Na, leading to the formation of radical anions.[9,12–13] Notably, our research group has demonstrated that when these reduction reactions were performed with electropositive rare-earth compounds, the resulting reduction products were unstable and could not be isolated.[14]

Over the past two decades, extensive research has been conducted on formazanate complexes based on main group elements, with a particular focus on compounds containing boron.[13,15–17] However, the literature regarding formazanate compounds of group 14 elements remains considerably limited, especially when compared to the well-explored chemistry of group 13 formazanate species. To the best of our knowledge, the only reported group 14 complexes are a series of hypercoordinated heavier group 14 neutral compounds and their radical anions.[18] These radical anions are analogues to verdazyl radicals and remained exceptionally stable even in the absence of significant steric bulk or other stabilizing effects (Scheme 1). Since then, no further research on formazanate chemistry related to group 14 elements has been reported.

In recent decades, the chemistry of low-valent group 14 compounds has undergone significant expansion. These compounds exhibit a distinctive dual Lewis acid-base character attributed to the presence of both a lone pair and a vacant p-orbital.[19–24] Consequently, they have garnered substantial interest, particularly regarding the capability to cleave both single bonds, such as R–H (R=H, C, N, O, etc.), and double bonds, such as C=X (X=C, N, O, etc.).[20,25–27]

Taking into account the redox-active nature of formazanates and the versatile reactivities of low-valent group 14 compounds, we decided to use both as starting materials to investigate their coordination and redox chemistry.

[a] D. Jin, Dr. X. Sun, V. R. Naina, Prof. Dr. P. W. Roesky
Institute of Inorganic Chemistry
Karlsruhe Institute of Technology (KIT)
Engesserstraße 15, 76131 Karlsruhe (Germany)
E-mail: roesky@kit.edu

Supporting information for this article is available on the WWW under https://doi.org/10.1002/chem.202301958

Special Collection Part of a Special Collection on the p-block elements.

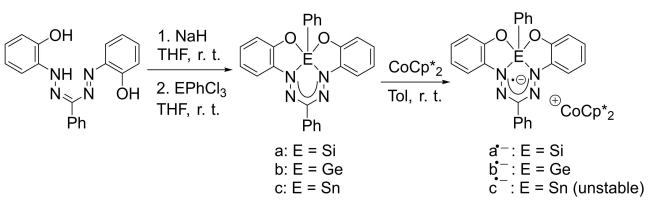

Scheme 1. Reported synthesis of hypercoordinated group 14 formazanate compounds (Cp* = pentamethylcyclopentadienide).[18]

Results and Discussion

The formazan ligand comprising *tert*-butyl substituent on the backbone [L^{tBu}H] (L^{tBu}=PhNNC(4-^{t}BuPh)NNPh) and its potassium salt [L^{tBu}K(thf)] were synthesized following previously reported methods.[14] Salt metathesis reactions of the [L^{tBu}K(thf)] with benzamidinate-supported chlorotetrylenes [L^{Ph}ECl] (L^{Ph}=PhC(^{t}BuN)$_2$, E=Si, Ge, Sn)[28–30] in THF at room temperature led to three different reaction pathways and the corresponding products **1**–**3** were isolated (Scheme 2).

In the reaction with the chlorosilylene, unexpected smooth oxidative addition of one formazanate N=N to both Si(II) centers resulted in the formation of compound **1** comprising a fused four-membered Si_2N_2 core and a five-membered NCN_2Si heterocycle. Formally, the reaction can be understood as a two-step process, in which one N=N bond is reduced to a N–N by one Si(II) atom followed by the oxidative addition of the newly formed N–N bond to the other Si(II) atom. Similar cleavage of the N–N bond in formazanate chemistry has thus far been observed primarily in boron compounds but under much harsher conditions involving reaction with Na reagent or heating.[15,31] Crystals of compound **1** with a red coloration were obtained through the diffusion of *n*-pentane into its toluene solution, resulting in its crystallization in the monoclinic space group $P2_1/n$. The molecular structure of compound **1** in the solid state is illustrated in Figure 1.

In compound **1**, the silicon atom Si1 is pentacoordinated by five nitrogen atoms in a distorted trigonal-pyramidal geometry, while atom Si2 is tetrahedrally coordinated by atoms N3, N4, an intact formazanate ligand in its 'open' κ^1(N)-form through N10 atom and the κ^1(N)-coordinated benzamidinate via N11 atom.

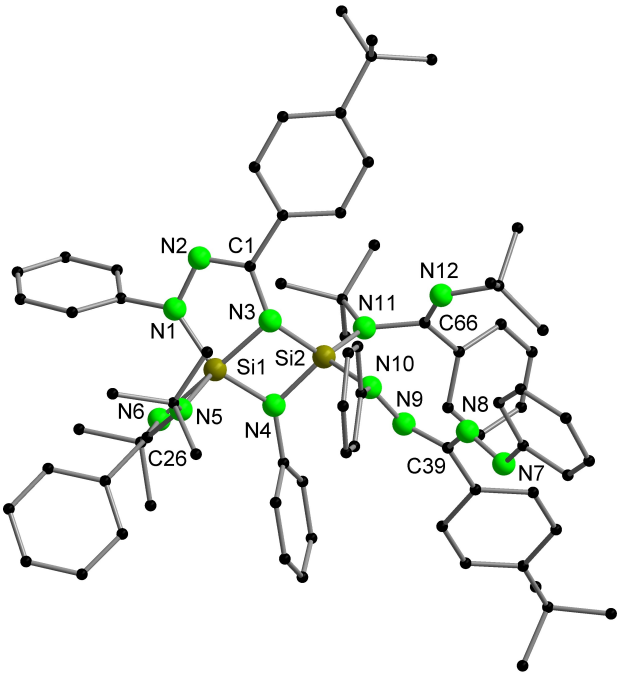

Figure 1. Molecular structure of **1** in the solid state. All hydrogen atoms are omitted for clarity. Selected bond lengths [Å] and bond angles [°]: Si1–N1 1.759(2), Si1–N3 1.833(2), Si1–N4 1.781(2), Si1–N5 1.844(2), Si1–N6 1.928(2), Si2–N3 1.717(2), Si2–N4 1.729(2), Si2–N10 1.766(2), Si2–N11 1.726(2), N1–N2 1.411(2), N7–N8 1.264(2), N9–N10 1.374(2), N2–C1 1.286(3), N3–C1 1.389(3), N5–C26 1.356(3), N6–C26 1.317(3), N8–C39 1.411(3), N9–C39 1.299(3), N11–C66 1.453(3), N12–C66 1.266(3); Si1–N3–Si2 95.42(8), Si1–N4–Si2 96.93(8), N10–Si2–N11 107.12(8), N1–Si1–N3 84.76(8), N3–Si1–N4 81.32(8), N3–Si2–N4 86.26(8), N5–Si1–N6 69.47(8), C39–N9–N10 123.5(2), N9–N10–Si2 107.31(12), C26–N5–Si1 92.96(13), C26–N6–Si1 90.47(13), N2–N1–Si1 116.15(13), C1–N2–N1 110.5(2), C1–N3–Si1 110.83(14), C1–N3–Si2 137.26(14), N5–C26–N6 107.1(2), N2–C1–N3 117.4(2), N8–C39–N9 120.3(2), N11–C66–N12 115.9(2), C66–N11–Si2 120.72(13).

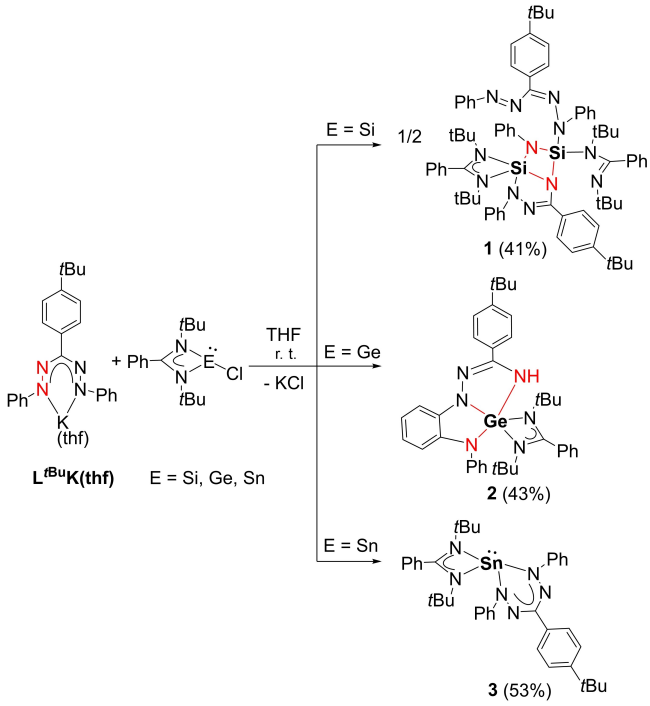

Scheme 2. Reactions of formazanate potassium salt with tetrylenes.

No matter in the cleaved or intact formazanate ligand moieties, the N–N and C–N bond distances are assigned to the corresponding double and single bonds, respectively. The bond lengths of Si1–N5 (1.844(2) Å) and Si1–N6 (1.928(2) Å) are comparable to those in the precursor [L^{Ph}SiCl].[32] All of the other Si–N bond distances (1.717(2) to 1.833(2) Å) are in the typical range for single bond lengths.[33] Both the four-membered (Si_2N_2) ring and five-membered ($SiCN_3$) ring exhibit virtually planar geometry, as evidenced by the sum of inner angles being 359.93° and 539.64°, respectively. In addition, both rings are oriented at a dihedral angle of 36.88° between their respective planes.

In comparison to the precursor [L^{Ph}SiCl] (δ (^{29}Si{^{1}H})= 14.6 ppm),[32] the ^{29}Si{^{1}H} NMR signals of compound **1** are upfield shifted to −45.8 and −102.3 ppm. The former signal could be assigned to the tetracoordinated Si atom, while the latter corresponds to the pentacoordinated Si atom. Furthermore, the ^{1}H NMR spectrum reveals the presence of multiple distinct sets of signals for the ^{t}Bu groups (Figure S1), in line with the asymmetric structure observed in the solid state. Some dynamic behaviour is seen in the ^{1}H NMR spectrum (Figure S2), which causes a superimposition of signals.

In the case of the reaction with the heavier chlorogermylene, a similar N=N bond cleavage and oxidation of the Ge center led to the formation of compound **2**. Remarkably, an anomalous C–H activation event occurred at one of the phenyl rings of the formazanate, resulting in the formation of a new C–N bond and the migration of H to N2. The precise mechanism of this process remains unclear. Interestingly, a comparable C–H activation and C–N bond formation was previously observed as a minor side product during the reduction of a formazanate boron compound, in which the aromatic homolytic substitution via a nitrogen-centered radical was proposed.[15,34] Another similar C–N bond formation in formazanate compounds has been reported via nucleophilic aromatic substitution of a C_6F_5-substituted formazan in the presence of a base.[35] Colorless crystals of compound **2** were obtained from a concentrated *n*-pentane solution and the molecular structure in the solid state is shown in Figure 2.

Compound **2** crystallizes in the triclinic space group $P\bar{1}$. The central Ge atom is pentacoordinated by five nitrogen atoms, with two nitrogen atoms from the benzamidinate ligand and three nitrogen atoms from the cleaved formazanate ligand. The newly formed phenylene entity, along with the derived formazanate is fused to two planar five-membered rings $GeCN_3$ and GeC_2N_2 through the Ge–N4 bond. The dihedral angle between the two five-membered planes is 31.77°. The almost equal bond distances of Ge–N1 (1.8726(15) Å), Ge–N2 (1.870(2) Å) and Ge–N4 (1.8771(14) Å) are comparable to the single bond lengths in the reported Ge-amidinate structures.[36] The bond length of C1–N2 (1.375(2) Å) is longer than that of C1–N3 (1.303(2) Å), representing a single bond and a double bond character, respectively.

In the ^{1}H NMR spectrum of compound **2**, the N*H* signal is observed at 5.38 ppm, consistent with its molecular structure. Two singlets at 1.27 and 0.75 ppm could be assigned to the ^{t}Bu groups of the formazanate and amidinate, respectively. Furthermore, the IR spectrum reveals a characteristic N–H stretching absorption at 3457 cm^{-1}, which aligns with the published value.[37–38]

The reactivity towards potassium formazanate exhibited a remarkable shift upon using the corresponding chlorostannylene. Rather than undergoing a redox reaction, a salt metathesis reaction resulted in the formation of heteroleptic stannylene compound **3**. Dark red plate-like single crystals of compound **3** were obtained from *n*-pentane solution. It crystallizes in the triclinic space group $P\bar{1}$ and the molecular structure in the solid state is shown in Figure 3.

In compound **3**, the tetracoordinated Sn atom, along with four nitrogen substituents, adopts a distorted square pyramidal geometry, with the Sn atom occupying the apical position. The presence of a stereochemically active lone pair on the opposite side of the Sn center forces both ligands to be oriented on the same side. The almost equal bond lengths of N–N and C–N in formazanate and benzamidinate ligands, indicate the significant delocalization of the negative charge in each ligand backbone.

In the ^{1}H NMR spectrum of **3**, two singlet signals corresponding to the ^{t}Bu groups are observed at 1.35 ppm and 0.96 ppm, which could be assigned to the formazanate and

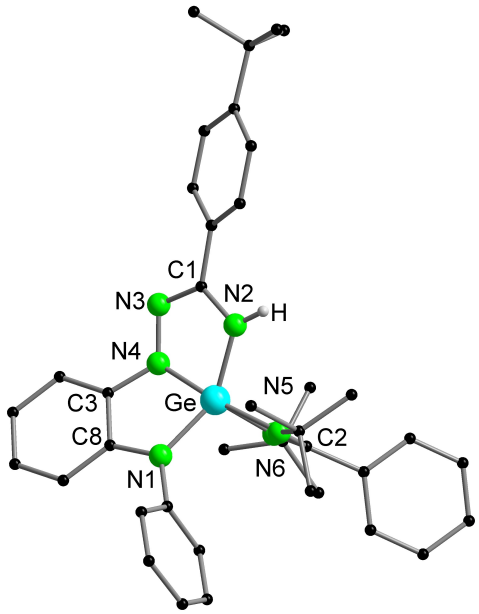

Figure 2. Molecular structure of **2** in the solid state. Hydrogen atoms (except N*H*) are omitted for clarity. Selected bond lengths [Å] and bond angles [°]: Ge–N1 1.8726(15), Ge–N2 1.870(2), Ge–N4 1.8771(14), Ge–N5 2.0034(14), Ge–N6 1.9467(15), N2–C1 1.375(2), N3–C1 1.303(2), N3–N4 1.393(2), N4–C3 1.384(2), N5–C2 1.324(2), N6–C2 1.336(2), N1–C8 1.399(2), C3–C8 1.426(2); N1–Ge–N2 144.39(7), N1–Ge–N4 85.16(6), N1–Ge–N5 99.73(6), N1–Ge–N6 107.04(6), N2–Ge–N4 80.76(7), N2–Ge–N5 93.99(6), N2–Ge–N6 108.57(7), N4–Ge–N5 174.67(6), N4–Ge–N6 114.23(6), N5–Ge–N6 66.51(6), C2–N5–Ge 91.07(10), N3–N4–Ge 117.66(11), C3–N4–Ge 114.89(11), C3–N4–N3 120.84(13), C1–N2–Ge 113.45(13), C8–N1–Ge 112.73(11), C2–N6–Ge 93.19(10), N4–C3–C8 112.04(14).

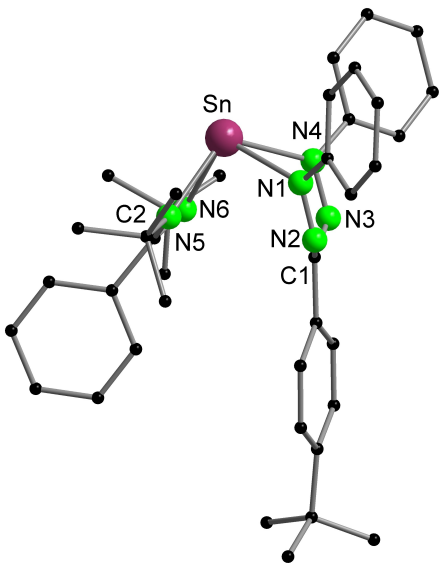

Figure 3. Molecular structure of **3** in the solid state. All hydrogen atoms are omitted for clarity. Selected bond lengths [Å] and bond angles [°]: Sn–N1 2.272(2), Sn–N4 2.344(2), Sn–N5 2.265(2), Sn–N6 2.235(2), N1–N2 1.314(2), N3–N4 1.306(2), N2–C1 1.342(3), N3–C1 1.343(3), N5–C2 1.318(2), N6–C2 1.333(2); N1–Sn–N4 63.78(6), N1–Sn–N5 82.86(6), N1–Sn–N6 107.25(6), N4–Sn–N5 118.03(6), N4–Sn–N6 82.49(6), N5–Sn–N6 58.59(6), N2–C1–N3 122.3(2), N5–C2–N6 112.3(2), N1–N2–C1 116.8(2), N2–N1–Sn 118.97(12), N4–N3–C1 117.3(2), N3–N4–Sn 118.73(13), C2–N5–Sn 93.74(12), C2–N6–Sn 94.65(12).

benzamidinate ligands, respectively. Both signals show a slight downfield shift compared with corresponding signals in compound **2**. In the $^{119}Sn\{^1H\}$ NMR spectrum, the resonance of compound **3** is detected at −499.9 ppm, which is significantly upfield shifted compared to the starting material stannylene [$L^{Ph}SnCl$] ($\delta = 29.6$ ppm)[30] and in agreement with the resonance of the homoleptic bis(guanidinato) tin(II) complex [{*p*Tol-NC[N-($SiMe_3$)$_2$]N-*p*Tol}$_2$Sn] ($\delta = -432.0$ ppm).[39]

Given the intriguing and smooth insertion of the chlorosilylene [$L^{Ph}SiCl$] into the N=N bond of the formazanate, we were motivated to explore this reactivity further. Consequently, we conducted a reaction between the neutral formazan ligand [$L^{tBu}H$] and the silylene [$L^{Ph}SiCl$]. This reaction led to the formation of compound **4**, where the anionic formazanate coordinates to the Si atoms (Scheme 3). We speculate that HCl elimination occurred during this reaction and a part of the chlorosilylene in the reaction mixture acted as a base to capture the HCl, as evidenced by the isolation of the side product [{PhC(^{t}BuN)$_2$H$_2$}Cl] several times. The structure of the side product is shown in Supporting Information (Figure S26) and its

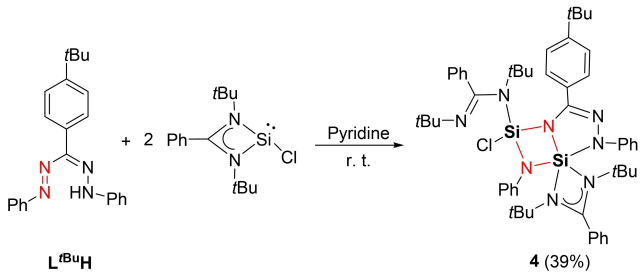

Scheme 3. Reaction of the neutral formazan ligand with silylene [$L^{Ph}SiCl$].

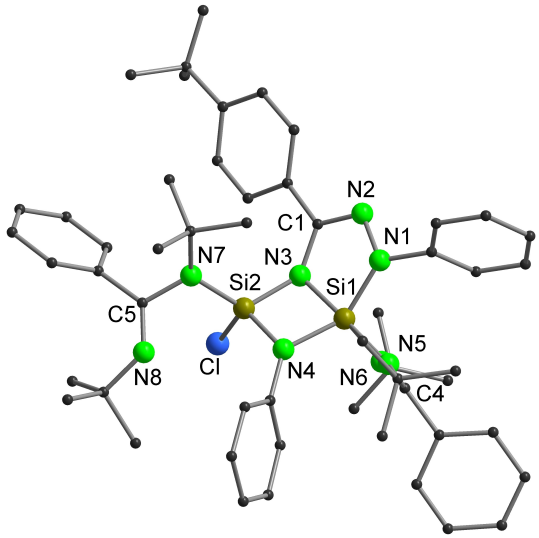

Figure 4. Molecular structure of **4** in the solid state. All hydrogen atoms are omitted for clarity. Selected bond lengths [Å] and bond angles [°]: Si2–Cl 2.088(2), Si1–N1 1.766(4), Si1–N3 1.806(4), Si1–N4 1.787(4), Si1–N5 1.837(4), Si1–N6 1.905(4), Si2–N3 1.696(4), Si2–N4 1.711(4), Si2–N7 1.711(4), N1–N2 1.428(5), N2–C1 1.299(6), N3–C1 1.379(6), N7–C5 1.425(6), N8–C5 1.272(6); N3–Si2–N4 86.4(2), N3–Si1–N4 81.0(2), N1–Si1–N3 84.3(2), Si1–N3–Si2 96.2(2), C1–N3–Si1 112.6(3), C1–N2–N1 108.7(4), N2–N1–Si1 116.6(3), N2–C1–N3 117.4(4), N7–C5–N8 115.8(4).

crystal characteristics match well with the published data.[40] To optimize the reaction conditions, pyridine was employed as a solvent to consume the generated HCl. As a result, the yield of compound **4** was increased, but the formation of side product could still be traced based on ^1H NMR analysis of the crude product.

Single crystals of **4** suitable for X-ray diffraction analysis were obtained by slow evaporation of its Et_2O solution at room temperature. Different from compound **1**, compound **4** crystallizes in the triclinic space group $P\bar{1}$ and its molecular structure is depicted in Figure 4. From the molecular structure, we can see that there is a striking similarity between compounds **1** and **4**. Compared with compound **1**, the intact formazanate is replaced by a Cl atom in compound **4**, while the other parts of the molecule are similar. As observed for **1**, compound **4** is also formed by the insertion of two Si(II) atoms into one N=N bond.

In the $^{29}Si\{^1H\}$ NMR spectrum of compound **4**, two distinct signals were observed at −63.3 ppm and −101.9 ppm. The former signal is upfield shifted when compared to compound **1** (−45.8 ppm) due to the coordination of Cl atom to the Si atom instead of N atom. The latter peak is similar to the resonance of the pentacoordinated Si atom in compound **1** (−102.3 ppm). In the ^1H NMR, signals of ^{t}Bu groups appeared as three singlets and could be clearly identified for the formazanate (1.23 ppm) and amidinate (1.11 and 0.92 ppm).

To avoid the HCl elimination, the pyridine-functionalized and chlorine-free silylene [$L^{Ph}SiNMePy$] (Py = pyridine)[41] was chosen as the precursor. An equimolar mixture of [$L^{Ph}SiNMePy$] and [$L^{tBu}H$] was reacted, leading to the isolation of compound **5** as colorless crystals with a yield of 41% (Scheme 4).

In this reaction, one of the N=N bonds was reduced and Si(IV) was formed. Interestingly, in contrast to aforementioned Si compounds **1** and **4**, no N–N bond cleavage was observed in this case. The successful isolation of compound **5** supports the hypothesis that the oxidative addition of the formazanate to two Si(II) atoms is a stepwise process as discussed in details for the formation of compound **1** (see above). It is worth noting that for formazan (with N*H*) supported complexes, there are only limited examples reported,[42–43] in contrast to the more extensive studies on anionic formazanate complexes.

The structure of compound **5** in the solid state was confirmed through X-ray diffraction analysis, as shown in Figure 5. It crystallizes in the monoclinic space group $P2_1/c$. The central Si atom is surrounded by five nitrogen atoms derived

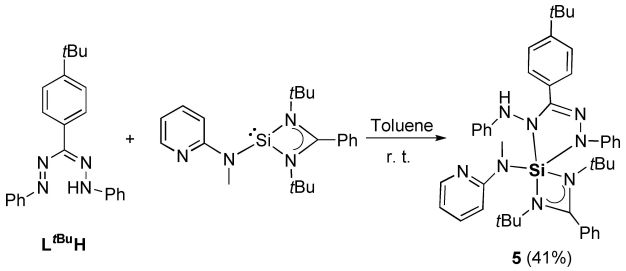

Scheme 4. Reaction of the neutral formazan ligand with silylene [$L^{Ph}SiNMePy$].

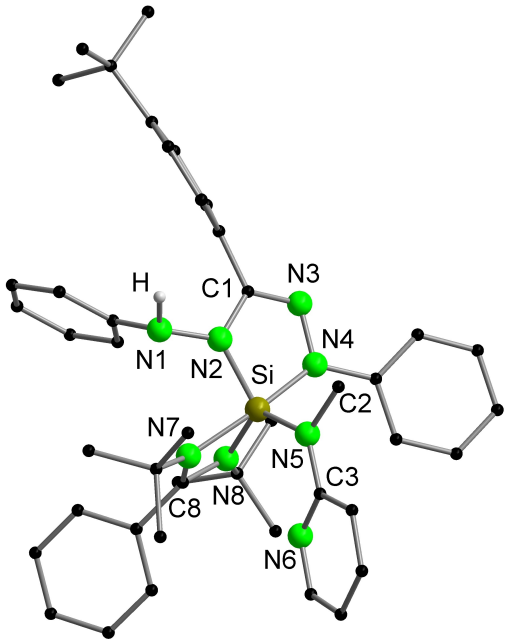

Figure 5. Molecular structure of **5** in the solid state. Hydrogen atoms (except N*H*) are omitted for clarity. Compound **5** crystallizes with two molecules in the asymmetric unit, the bonding angle and distances are similar, thus only one molecule is depicted here. Selected bond lengths [Å] and bond angles [°]: Si–N2 1.7558(11), Si–N4 1.8101(12), Si–N5 1.7693(13), Si–N7 1.9408(11), Si–N8 1.8334(11), N1–N2 1.4190(15), N3–N4 1.4068(15), N2–C1 1.405(2), N3–C1 1.289(2); N2–Si–N4 83.76(5), N7–Si–N8 69.15(5), C1–N2–Si 113.83(8), C1–N2–N1 117.78(11), C1–N3–N4 109.06(11), N3–N4–Si 115.98(8), N1–N2–Si 126.66(9), N2–C1–N3 116.72(12).

from the ligands and its coordination geometry can be best described as a distorted trigonal bipyramidal. The formally negatively charged formazanate ligand coordinates to the Si atom in a bidentate fashion via internal atom N2 and terminal atom N4, generating a five-membered chelate. The bond lengths of the N–N and N–C within the formazan backbone are consistent with those observed for the 5-membered chelate rings in formazanate compounds **1** and **4**.

The presence of the N*H* moiety in compound **5** was confirmed by the observation of a singlet resonance at 5.63 ppm in the ^{1}H NMR spectrum, which is consistent with the N*H* resonance observed in compound **2**. The asymmetric molecular structure of compound **5** was evidenced by the presence of two distinct singlet signals at 1.18 and 0.76 ppm, corresponding to the ^{t}Bu substituents of the benzamidinate ligand. The ^{t}Bu group of the formazanate ligand exhibited a signal at 1.42 ppm, which is slightly downfield shifted compared to its position in compound **4**. In the IR spectrum, an absorption band corresponding to the N–H stretching vibration was observed at 3353 cm^{-1}, which is in agreement with the N–H stretching frequency observed in the Ge compound **2**.

The successful synthesis of complex **5** highlights the potential of using neutral formazan ligands in the coordination chemistry with silylenes. However, when [L$^{t\text{Bu}}$H] was reacted with the germylene [L$^{\text{Ph}}$GeCl], a tetrazolium cation was formed (see Supporting Information, Figure S27).[44] We performed no further investigation on this compound. Meanwhile, there was no reactivity was observed between [L$^{t\text{Bu}}$H] and [L$^{\text{Ph}}$SnCl], which is rational due to the lower reactivities of the heavier tetrylenes. These observations provide basic insights into the reactivity patterns of formazan ligands with different tetrylene compounds.

Conclusions

In conclusion, a series of reactions of formazanate or formazan with low valent group 14 compounds were explored. These reactions showcased various reactivity patterns, including N=N bond cleavage, Si or Ge insertion into the N=N bond, C–H activation of a phenyl group, as well as substitution and addition reactions. This work expanded our understanding of the diverse redox chemistry of formazanate ligands and provided more valuable insights into the formazanate coordination chemistry.

Experimental Section

Experimental details are given in the Supporting Information, including starting materials, characterization methods, experimental procedures, full spectroscopic data for all new compounds, copies of ^{1}H, ^{13}C{^{1}H}, ^{29}Si{^{1}H}, ^{119}Sn{^{1}H} NMR spectra, IR spectra, elemental analyses, and crystallographic data.

Deposition Numbers 2270922 (for **1**), 2270923 (for **2**), 2270924 (for **3**), 2270925 (for **4**), and 2270926 (for **5**) contain the supplementary crystallographic data for this paper. These data are provided free of charge by the joint Cambridge Crystallographic Data Centre and Fachinformationszentrum Karlsruhe Access Structures service.

The authors have cited additional references within the Supporting Information.[45–47]

Acknowledgements

D.J. thanks the China Scholarship Council and KIT for generous support. V.R.N. acknowledges GRK 2039 Molecular Architectures for Fluorescent Cell Imaging for the financial support. We also acknowledge Prof. Dr. D. Fenske for data collection on a Stoe StadiVari diffractometer with Ga-metal-jet source within the Karlsruhe Nano Micro Facility (KNMFi). Open Access funding enabled and organized by Projekt DEAL.

Conflict of Interests

The authors declare no conflict of interest.

Data Availability Statement

The data that support the findings of this study are available in the supplementary material of this article.

Keywords: bond activation · coordination chemistry · formazanate/formazan · redox reactivity · tetrylenes

[1] G. Moss, P. Smith, D. Tavernier, *Pure Appl. Chem.* **1995**, *67*, 1307–1375.
[2] M. Szymczyk, A. El-Shafei, H. S. Freeman, *Dyes Pigm.* **2007**, *72*, 8–15.
[3] S. A. Khan, S. Shahid, S. Kanwal, K. Rizwan, T. Mahmood, K. Ayub, *J. Mol. Struct.* **2019**, *1175*, 73–89.
[4] M. E. Khalifa, E. A. Elkhawass, A. Pardede, M. Ninomiya, K. Tanaka, M. Koketsu, *Monatsh. Chem.* **2018**, *149*, 2195–2206.
[5] N. M. Aljamali, *Int. J. Polym. Sci.* **2021**, *7*, 5–14.
[6] S. A. Khan, K. Rizwan, S. Shahid, M. A. Noamaan, T. Rasheed, H. Amjad, *Appl. Organomet. Chem.* **2020**, *34*, 5444.
[7] J. C. Stockert, R. W. Horobin, L. L. Colombo, A. Blázquez-Castro, *Acta Histochem.* **2018**, *120*, 159–167.
[8] L. Bourget-Merle, M. F. Lappert, J. R. Severn, *Chem. Rev.* **2002**, *102*, 3031–3066.
[9] D. L. Broere, B. Q. Mercado, J. T. Lukens, A. C. Vilbert, G. Banerjee, H. M. Lant, S. H. Lee, E. Bill, S. Sproules, K. M. Lancaster, *Chem. Eur. J.* **2018**, *24*, 9417–9425.
[10] R. Mondol, E. Otten, *Inorg. Chem.* **2019**, *58*, 6344–6355.
[11] M. C. Chang, T. Dann, D. P. Day, M. Lutz, G. G. Wildgoose, E. Otten, *Angew. Chem. Int. Ed.* **2014**, *53*, 4118–4122.
[12] J. B. Gilroy, M. J. Ferguson, R. McDonald, B. O. Patrick, R. G. Hicks, *Chem. Commun.* **2007**, 126–128.
[13] R. Mondol, D. A. Snoeken, M.-C. Chang, E. Otten, *Chem. Commun.* **2017**, *53*, 513–516.
[14] D. Jin, X. Sun, A. Hinz, P. W. Roesky, *Dalton Trans.* **2022**, *51*, 5218–5226.
[15] M.-C. Chang, E. Otten, *Inorg. Chem.* **2015**, *54*, 8656–8664.
[16] S. M. Barbon, V. N. Staroverov, J. B. Gilroy, *Angew. Chem. Int. Ed.* **2017**, *56*, 8173–8177.
[17] J. B. Gilroy, E. Otten, *Chem. Soc. Rev.* **2020**, *49*, 85–113.
[18] R. R. Maar, S. D. Catingan, V. N. Staroverov, J. B. Gilroy, *Angew. Chem. Int. Ed.* **2018**, *57*, 9870–9874.
[19] M. Asay, C. Jones, M. Driess, *Chem. Rev.* **2011**, *111*, 354–396.
[20] S. K. Mandal, H. W. Roesky, *Acc. Chem. Res.* **2012**, *45*, 298–307.
[21] J. Schneider, K. M. Krebs, S. Freitag, K. Eichele, H. Schubert, L. Wesemann, *Chem. Eur. J.* **2016**, *22*, 9812–9826.
[22] Y. Mizuhata, T. Sasamori, N. Tokitoh, *Chem. Rev.* **2009**, *109*, 3479–3511.
[23] L. Alvarez-Rodriguez, J. A. Cabeza, P. Garcia-Alvarez, D. Polo, *Coord. Chem. Rev.* **2015**, *300*, 1–28.
[24] N. Tokitoh, R. Okazaki, *Coord. Chem. Rev.* **2000**, *210*, 251–277.
[25] T. Chu, G. I. Nikonov, *Chem. Rev.* **2018**, *118*, 3608–3680.
[26] T. J. Hadlington, M. Driess, C. Jones, *Chem. Soc. Rev.* **2018**, *47*, 4176–4197.
[27] Y. P. Zhou, M. Driess, *Angew. Chem. Int. Ed.* **2019**, *58*, 3715–3728.
[28] S. S. Sen, H. W. Roesky, D. Stern, J. Henn, D. Stalke, *J. Am. Chem. Soc.* **2010**, *132*, 1123–1126.
[29] S. Nagendran, S. S. Sen, H. W. Roesky, D. Koley, H. Grubmüller, A. Pal, R. Herbst-Irmer, *Organometallics* **2008**, *27*, 5459–5463.
[30] S. S. Sen, M. P. Kritzler-Kosch, S. Nagendran, H. W. Roesky, T. Beck, A. Pal, R. Herbst-Irmer, *Eur. J. Inorg. Chem.* **2010**, 5304–5311.
[31] M. C. Chang, E. Otten, *Organometallics* **2016**, *35*, 534–542.
[32] C. W. So, H. W. Roesky, J. Magull, R. B. Oswald, *Angew. Chem. Int. Ed.* **2006**, *45*, 3948–3950.
[33] M. Ippolito, S. Meloni, *Phys. Rev. B* **2011**, *83*, 165209.
[34] W. R. Bowman, J. M. Storey, *Chem. Soc. Rev.* **2007**, *36*, 1803–1822.
[35] R. Travieso-Puente, S. Budzak, J. Chen, P. Stacko, J. T. Jastrzebski, D. Jacquemin, E. Otten, *J. Am. Chem. Soc.* **2017**, *139*, 3328–3331.
[36] J. A. Cabeza, P. García-Álvarez, E. Pérez-Carreño, D. Polo, *Chem. Eur. J.* **2014**, *20*, 8654–8663.
[37] A. Jana, S. S. Sen, H. W. Roesky, C. Schulzke, S. Dutta, S. K. Pati, *Angew. Chem. Int. Ed.* **2009**, *48*, 4246–4248.
[38] Z. D. Brown, J.-D. Guo, S. Nagase, P. P. Power, *Organometallics* **2012**, *31*, 3768–3772.
[39] T. Chlupaty, Z. Padelkova, F. DeProft, R. Willem, A. Ruzicka, *Organometallics* **2012**, *31*, 2203–2211.
[40] L. Alvarez-Rodriguez, J. A. Cabeza, P. Garcia-Alvarez, D. Polo, *Organometallics* **2015**, *34*, 5479–5484.
[41] X. Qi, T. Zheng, J. Zhou, Y. Dong, X. Zuo, X. Li, H. Sun, O. Fuhr, D. Fenske, *Organometallics* **2019**, *38*, 268–277.
[42] L. Capulín Flores, L. A. Paul, I. Siewert, R. Havenith, N. Zúñiga-Villarreal, E. Otten, *Inorg. Chem.* **2022**, *61*, 13532–13542.
[43] M.-C. Chang, P. Roewen, R. Travieso-Puente, M. Lutz, E. Otten, *Inorg. Chem.* **2015**, *54*, 379–388.
[44] D. G. Golovanov, D. S. Perekalin, A. A. Yakovenko, M. Y. Antipin, K. A. Lyssenko, *Mendeleev Commun.* **2005**, *15*, 237–239.
[45] G. Sheldrick, *Acta Crystallogr. Sect. A* **2008**, *64*, 112–122.
[46] G. Sheldrick, *Acta Crystallogr. Sect. C* **2015**, *71*, 3–8.
[47] O. V. Dolomanov, L. J. Bourhis, R. J. Gildea, J. A. K. Howard, H. Puschmann, *J. Appl. Crystallogr.* **2009**, *42*, 339–341.

Manuscript received: June 20, 2023
Accepted manuscript online: July 27, 2023
Version of record online: ■■, ■■

RESEARCH ARTICLE

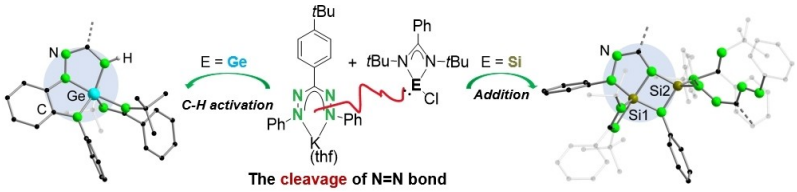

The diverse redox chemistry of formazanate/formazan with low-valent group 14 compounds is inverstigated. Both formazanate potassium salt and neutral formazan ligands were subjected to reactions with tetrylenes. In the former case, the anticipated salt metathesis reactions occurred, accompanied by unexpected reduction/insertion and C–H activation. The latter reactions displayed substitution and addition reaction patterns.

*D. Jin, Dr. X. Sun, V. R. Naina, Prof. Dr. P. W. Roesky**

1 – 7

Diverse Reactions of Formazanate/Formazan with Tetrylenes: Reduction, C–H Bond Activation, Substitution and Addition